Article

Not peer-reviewed version

Genome-Wide Identification, Cloning and Expression Analysis of *DFR* Gene Family in *Lonicera japonica* Thunb. under Drought and Salt Stress

Dandan Lu , Xiaoyu Su , Yao Sun , Lei Li , Yongliang Yu , Chunming Li , Yiwen Cao , Lina Wang , Meiyu Qiao , Hongqi Yang , Mengfan Su , Zhengwei Tan * , Huizhen Liang *

Posted Date: 20 November 2025

doi: 10.20944/preprints202511.1484.v1

Keywords: *Lonicera japonica* Thunb.; DFR gene family; anthocyanin; gene cloning and expression analysis; drought and salt stress; flower color formation

 doi:10.20944/preprints202511.1484.v1

Article

Genome-Wide Identification, Cloning and Expression Analysis of *DFR* Gene Family in *Lonicera japonica* Thunb. under Drought and Salt Stress

Dandan Lu [1,2], Xiaoyu Su [1,2], Yao Sun [1,2], Lei Li [1,2], Yongliang Yu [1,2], Chunming Li [1,2], Yiwen Cao [1,2], Lina Wang [1,2], Meiyu Qiao [1,2], Hongqi Yang [1,2], Mengfan Su [1,2], Zhengwei Tan [1,2,*] and Huizhen Liang [1,2,*]

[1] Institute of Chinese Herbal Medicines, Henan Academy of Agricultural Sciences, Zhengzhou 450002, China
[2] Provincial Key Laboratory of Conservation and Utilization of Traditional Chinese Medicine Resources, Zhengzhou, Henan, 450002, China
* Correspondence: zhwtan@126.com (Z.T.); lhzh66666@163.com (H.L.)

Abstract

Based on the genome and transcriptome data of *Lonicera japonica* Thunb., this study identified six *LjDFR* gene family members at the genome-wide level. These genes were located on Chr.04 and Chr.09, and the full-length coding sequences of LjDFR1 to LjDFR6 were successfully cloned. The proteins encoded by the cloned genes are all hydrophilic, with secondary structures dominated by α-helices and random coils. The subcellular localization analysis indicated that LjDFRs are primarily localized in the cell membrane and nucleus. Phylogenetic analysis classified the LjDFR proteins into four subfamilies, clustering with DFR homologs from species such as *Capsicum annuum* and *Camellia sinensis*, reflecting a high degree of evolutionary conservation. Promoter analysis identified multiple cis-acting elements associated with light response, hormone signaling, and stress-responses. Expression pattern analysis demonstrated that *LjDFR* genes exhibit tissue-specific and stage-specific expression patterns during flower development in *L. japonica* varieties with different floral colors. Notably, *LjDFR2* expression was significantly higher in the deeply pigmented tissues of *Lonicera japonica* Thunb. var. *chinensis* (Wats.) Bak. than in L. japonica. Together with its phylogenetic clustering with the anthocyanin-related *CsDFRa* and *CaDFR5* genes, this finding suggests that *LjDFR2* potentially positively correlated with anthocyanin accumulation. Furthermore, the expression of *LjDFR2* and *LjDFR4* was significantly induced under both drought and salt stress, indicating their involvement in abiotic stress responses. This study provides a foundation for further functional characterization of *LjDFR* genes in anthocyanin metabolism and stress resistance, and offers valuable candidate genes for molecular breeding of *L. japonica*.

Keywords: *Lonicera japonica* Thunb.; DFR gene family; anthocyanin; gene cloning and expression analysis; drought and salt stress; flower color formation

1. Introduction

Anthocyanins are a class of water-soluble pigments widely present in plants, belonging to flavonoid-derived secondary metabolites. They are extensively distributed in the vacuoles of plant organs such as flowers, fruits, seeds, and leaves [1]. In plants, anthocyanins serve multiple important functions, including attracting pollinating insects, deterring herbivores, activating chemical defenses, and providing protection against pathogen infections, ultraviolet radiation, low temperatures, and drought [2]. Due to their significant antioxidant properties, anthocyanins also offer multiple health benefits to animals and humans, such as regulating blood glucose levels, lowering blood lipids, and inhibiting the occurrence of certain cancers [3]. Currently, approximately 600 types of anthocyanins have been identified in nature, with six main types: delphinidin, pelargonidin, petunidin, cyanidin,

 doi:10.20944/preprints202511.1484.v1

peonidin, and malvidin. Among these, cyanidin is the most common. In terms of plant coloration, cyanidin and pelargonidin impart red hues, while delphinidin and its methylated derivatives (e.g., petunidin and malvidin) confer blue-purple colors [4]. The final color displayed by anthocyanins is collectively influenced by various factors such as copigmentation, vacuolar pH, structural differences, and metal ions [5].

The biosynthetic pathway of anthocyanins is a specific branch of the flavonoid biosynthetic pathway and is the end product of the phenylpropanoid/flavonoid pathway, involving multiple enzymes [6]. Dihydroflavonol 4-reductase (DFR) is the rate-limiting enzyme in this pathway. It determines the direction of carbon flow, leading to significant differences in the types of anthocyanins [7]. Studies have shown that DFR can catalyze three colorless dihydroflavonols (dihydrokaempferol DHK, dihydroquercetin DHQ, dihydromyricetin DHM) into the corresponding leucoanthocyanidins. Therefore, DFR is regarded as a key regulatory node in the process of anthocyanin biosynthesis [8]. There are three types of DFRs: The first is the Asparagine-type (Asn-type) DFRs, with Asn at position 134, widely distributed in plants, capable of catalyzing the conversion of all three dihydroflavonols; the second is the Aspartate-type (Asp-type) DFRs, with Asp at position 134, highly specific for DHQ and DHM, and cannot effectively catalyze DHK; the third type is called non-Asn/Asp-type DFRs, containing neither Asn nor Asp [9]. Biochemical analyses indicate that DFR proteins have substrate specificity, which influences the content and proportion of different anthocyanins, ultimately leading to variations in plant color [10]. For example, petunia DFR cannot effectively catalyze the monohydroxylated DHK, hence this species lacks orange flowers. However, when several amino acids at the active site of the DFR enzyme are modified, the mutated petunia DFR gains the ability to catalyze DHM, resulting in orange flowers producing pelargonidin-based anthocyanins [11]. Consequently, DFR plays a crucial role in the anthocyanin pathway, and modulating its expression level can effectively alter plant color.

Lonicera japonica Thunb. (Caprifoliaceae) refers to the dried flower buds or nearly open flowers of the plant, commonly known as Jin-Yin-Hua, or Flos Lonicerae Japonicae (FLJ). It is a traditional Chinese medicinal herb with biological activities such as antibacterial, anti-inflammatory, antiviral, antioxidant, anti-endotoxin, hypolipidemic, and antipyretic effects [12]. Pharmacological studies have shown that its main active components include chlorogenic acid, luteolin-7-O-glucoside (luteoloside), and iridoid compounds, which can be used to treat arthritis, diabetes, fever, infections, ulcers, and swelling. Additionally, it is an important antiviral agent against SARS coronavirus, influenza A virus, and the novel coronavirus [13]. *Lonicera japonica* Thunb. var. *chinensis* (Wats.) Bak. (RFLJ) is a natural mutant of L. japonica. Its young branches, leaves, and stems are all purplish-red, and the corolla is purplish-red on the outside and white on the inside. Compared to L. japonica, RFLJ contains higher levels of luteoloside, quercetin, chlorogenic acid, and anthocyanins, as well as a greater variety of volatile oils. Research by Yuan et al. indicate that the anthocyanin content in RFLJ can be as high as 100 mg/100 g [14]. Consequently, RFLJ is more fragrant, has a longer flowering period, blooms earlier, and exhibits higher ornamental and tea-drinking value, integrating medicinal, ornamental, and greening purposes, along with stronger cold resistance and drought tolerance. L. japonica flowers exhibit vivid coloration and a sweet scent, progressing through six developmental stages: S1 (young alabastrum), S2 (green alabastrum), S3 (slightly white alabastrum), S4 (whole white alabastrum), S5 (silvery flower), and S6 (golden flower). Differential anthocyanin accumulation and flower color at S4 distinguish L. japonica (GFLJ, with green flower) from RFLJ (with purple flower) [15].

Currently, research on DFR mainly focuses on gene cloning and functional identification. The *DFR* gene family has been identified in only a few species, such as *Capsicum annuum* [16] and *Camellia sinensis* [17], while a comprehensive identification or systematic study of the *DFR* gene family in L. japonica has been lacking. In this study, based on the genome and transcriptome databases of L. japonica, we identified members of the LjDFR family at the whole-genome level and cloned all LjDFR members. We systematically analyzed their physicochemical properties, chromosomal localization, collinearity, evolutionary relationships, conserved protein domains, gene structures, and promoter

 doi:10.20944/preprints202511.1484.v1

cis-acting elements. Additionally, the subcellular localization of LjDFR proteins was verified using GFP fusion protein expression method, and the expression patterns of *LjDFR* genes in different tissues, at different flowering stages of varieties with different flower colors, and under drought and salt stresses were detected via qRT-PCR. This research lays a foundation for further exploring the function of *LjDFR* genes in the anthocyanin metabolic pathway and provides theoretical guidance for the breeding of new *Lonicera* varieties.

2. Materials and Methods

2.1. Materials and Stress Treatments

The test materials, GFLJ and RFLJ, were provided by the Institute of Chinese Herbal Medicines, Henan Academy of Agricultural Sciences, and cultivated under natural conditions at the Modern Agricultural Research and Development Base of Henan Academy of Agricultural Sciences. During the first flowering stage, roots, stems, leaves, and flower buds from both varieties were collected, along with flowers at different developmental stages. For each sample, 3 biological replicates were prepared. After rapid freezing in liquid nitrogen, samples were stored at -80 °C for subsequent use.

One-year-old healthy cutting seedlings were selected and acclimated to hydroponic culture using 50% Hoagland nutrient solution followed by 100% Hoagland nutrient solution, each for two weeks. Seedlings with uniform growth were then subjected to drought stress (25% PEG 6000) or salt stress (300 mmol·L^{-1} NaCl). Samples were collected at 0, 3, 12, 24, 48, and 80 hours after treatment initiation, with the 0-hour sample serving as the control. For each treatment, leaves from 3–5 seedlings were pooled to form one biological replicate. The mixed samples were quickly frozen in liquid nitrogen and stored at -80 °C, three replicates were taken for each time point. The experiment was conducted in a constant-temperature light incubator under the following conditions: temperature (23±2) °C, relative air humidity 40%–50%, light intensity 1,000 μmol·m^{-2}·s^{-1}, and a photoperiod of 14 h·d^{-1}.

2.2. Identification and Chromosomal Distribution of the LjDFR Gene Family

The L. japonica genome sequences, protein sequences, and genome annotation files (Project ID: PRJCA001719) were downloaded from the National Genomics Data Center (https://bigd.big.ac.cn/gwh, accessed on 21 October 2025)[18]. *Arabidopsis thaliana* DFR protein sequences were obtained from TAIR (https://www.arabidopsis.org/, accessed on 21 October 2025), while the DFR protein sequences of *Capsicum annuum*, *Camellia sinensis*, and *Brassica napus* were retrieved from the literature [16]. The AtDFR protein sequences were used for a BLASTP search against the L. japonica database. Sequences with homology greater than 50%, E-value less than 1×10^{-50}, and bit-score greater than 300 were screened, and duplicates were removed. Two online databases—SMART (http://smart.emblheidelberg.de/, accessed on 22 October 2025) and CD-Search Tool (https://www.ncbi.nlm.nih.gov/Structure/bwrpsb/bwrpsb.cgi, accessed on 22 October 2025) were used for verification, and sequences lacking the complete DFR conserved domain were excluded. Chromosomal location information of *LjDFR* genes was acquired from the genome annotation file (GFF), and the distribution was visualized using TBtools software.

2.3. Cloning, Physicochemical Properties, and Structural Characteristics Analysis of LjDFR Genes

Using the previously obtained *LjDFR* gene sequences as references, specific primers were designed with Primer Premier 5 software (Table S1). PCR amplification was performed using KOD enzyme with cDNA from L. japonica petals as the template. The 20 μL reaction system consisted of: 10 μL of 2×PCR buffer for KOD FX, 4 μL of 2 mM dNTPs, 2 μL of cDNA template, 0.6 μL each of forward and reverse primers, 0.4 μL of KOD FX, and 2.4 μL of sterile double-distilled water. The reaction program was set as follows: pre-denaturation at 94 °C for 2 min; 35 cycles of denaturation at 98 °C for 10 s, annealing at 55 °C for 30 s, and extension at 68 °C for 2 min; and a final extension at

 doi:10.20944/preprints202511.1484.v1

68 °C for 5 min. PCR products were ligated into a T-vector and sent to Henan Youkang Biotechnology for sequencing [19]. The obtained nucleotide sequences were imported into DNAMAN 6.0 to derive the encoded amino acid sequences. Physicochemical properties of LjDFR proteins, such as number of amino acids, molecular weight, theoretical isoelectric point and hydrophilicity/hydrophobicity were predicted using the Protein Parameter Calc tool in TBtools-II v2.202. Subcellular localization was predicted via Plant-mPLoc (http://www.csbio.sjtu.edu.cn/bioinf/plant-multi/, accessed on 23 October 2025). Secondary structure was predicted using Prabi (https://npsa-prabi.ibcp.fr/cgi-bin/npsa_automat.pl?page=/NPSA/npsa_sopma.html, accessed on 23 October 2025). Based on the principle of homology modeling, the tertiary structure models were constructed using SWISS-MODEL (https://swissmodel.expasy.org/interactive, accessed on 24 October 2025). Transmembrane domains were analyzed with TMHMM-2.0 (https://services.healthtech.dtu.dk/services/TMHMM-2.0/, accessed on 24 October 2025).

2.4. Subcellular Localization Analysis

Using the full-length plasmid obtained above as the template, the coding sequences of LjDFR3 and LjDFR6 without stop codons were amplified using primers with homologous arms and adapters. They were fused with the pCAMBIA1300 vector, and the 35S::LjDFR::GFP fusion vectors driven by the CaMV35S promoter were constructed using the ClonExpress® II One-Step Cloning Kit (Vazyme, Nanjing, China). The fusion vectors were transformed into the abaxial side of 3-week-old tobacco (*Nicotiana benthamiana*) leaves via *Agrobacterium tumefaciens* strain GV3101. Tobacco plants were cultured in the dark at 25 °C for 24 h, then grown normally for 1–2 days. A Zeiss LSM710 confocal laser scanning microscope was used to observe fluorescence signals with 488 excitation light.

2.5. Multiple Sequence Alignment and Phylogenetic Analysis

Multiple sequence alignment of DFR proteins from L. japonica, *Arabidopsis thaliana*, *Capsicum annuum*, *Camellia sinensis*, and *Brassica napus* was performed using ClustalW in MEGA 7.0 software. A phylogenetic tree was constructed using the Neighbor-joining method with Bootstrap set to 1,000. The tree was optimized using Evolview online software and Adobe Illustrator. Multiple sequence alignment of LjDFR proteins was conducted using DNAMAN6.0 and visualized with GeneDoc and Adobe Illustrator.

2.6. Conserved Motif and Gene Structure Analysis

The amino acid sequences of LjDFR proteins were submitted to the online tool MEME 5.5.2 (http://meme-suite.org/tools/meme, accessed on 24 October 2025) for conserved motif analysis (maximum number of motifs = 10, motif width = 6–50 amino acids). The exon-intron structure of *LjDFR* genes was analyzed using GSDS 2.0 (http://gsds.gao-lab.org/, accessed on 24 October 2025), and results were visualized using TBtools [20].

2.7. Collinearity Analysis and Identification of Cis-Acting Elements in Promoters of the LjDFR Gene Family

The collinear relationships among *LjDFR* gene family in the L. japonica genome were analyzed using One Step MCScanX [21] in TBtools and visualized via the Advance Circos module. The 2,000 bp sequences upstream of the ATG start codon of *LjDFR* genes were extracted from the L. japonica database. Cis-acting elements analysis was performed using PlantCARE (https://bioinformatics.psb.ugent.be/webtools/plantcare/html/, accessed on 24 October 2025), and the screened cis-acting regulatory elements were visualized using TBtools .

2.8. RNA Extraction, cDNA Synthesis, and qRT-PCR Analysis

Total RNA was extracted from roots, stems, leaves, flowers at different developmental stages, and stress-treated samples of both L. japonica varieties using the Vazyme FastPure® Universal Plant Total RNA Isolation Kit (Cat. No. RC411). RNA quality and integrity were assessed by 1.1% agarose

 doi:10.20944/preprints202511.1484.v1

gel electrophoresis, and concentration/purity were determined using a NanoDrop 2000 spectrophotometer. Total RNA (1 μg) with an A260/A280 ratio of 1.8–2.0 was selected for reverse transcription to synthesize cDNA using the Vazyme HiScript® Ⅲ 1st Strand cDNA Synthesis Kit (+gDNA wiper) (Cat. No. R312). Fluorescent quantitative primers were designed using Primer Premier 5 based on conserved regions of the cDNA sequences (Table S1). The 10 μL qRT-PCR reaction system consisted of 5 μL of RealStar Fast SYBR qPCR Mix (2×) (GenStar), 1 μL of cDNA (10×), 0.3 μL each of forward and reverse primers (10 μmol·L^{-1}), and 3.4 μL of RNase-free ddH_2O. The reaction program was: pre-denaturation at 95 °C for 2 min; 40 cycles of denaturation at 95 °C for 15 s and annealing/extension at 60 °C for 30 s. Amplification was performed on a QIAquant 96 2 plex real-time Detection System (Qiagen, Germany), and amplification specificity was monitored via melting curve analysis. Three biological replicates and three technical replicates were used. LjG6PD was used as the reference gene [22], and relative expression levels were calculated using the $2^{-\Delta\Delta CT}$ method. The experimental data are presented as mean ± standard deviation (SD) of three biological replicates. Tukey's test was used for significance analysis ($P< 0.05$; $P< 0.01$).

3. Results

3.1. Genome-Wide Identification, Full-length Cloning, and Chromosomal Distribution of LjDFR Gene Family

A total of 6 *DFR* genes were identified in L. japonica. Chromosomal localization analysis based on the genomic annotation information of the 9 chromosomes of L. japonica showed that these genes are distributed on Chr.04 and Chr.09 (Figure 1A). Among them, *LjDFR1*, *LjDFR2*, and *LjDFR5* are located on Chr.04, while *LjDFR3*, *LjDFR4*, and *LjDFR6* are located on Chr.09.

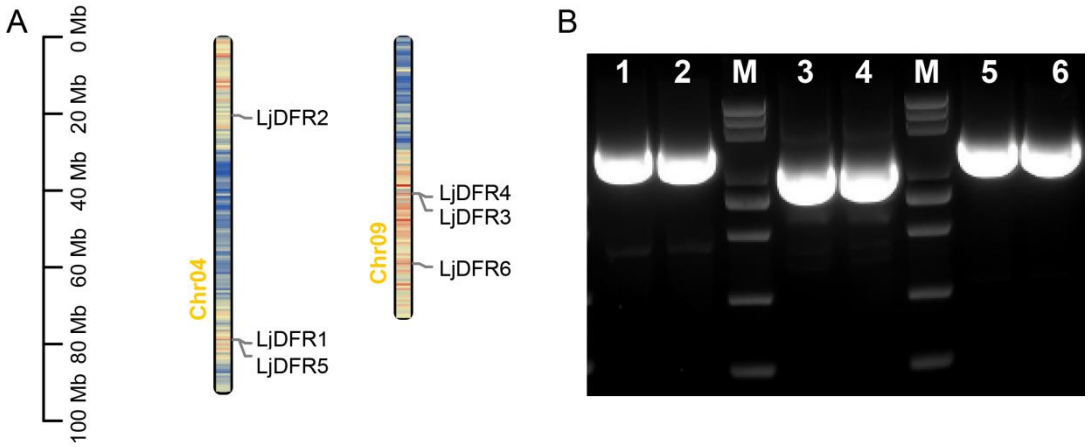

Figure 1. Distribution of *LjDFR* family members on chromosomes map (**A**) and PCR amplification of *LjDFR* genes (**B**). 1-6: LjDFR1-LjDFR6; M: DL 5000 marker (5000, 3000, 2000, 1000, 750, 500, 250, 100 bp).

To ensure the accuracy of subsequent bioinformatics analysis, we cloned all six *LjDFR* genes (Figure 1B) using cDNA from L. japonica petals, and then the products were ligated into T-vectors for sequencing. The sequencing results showed 93.62% to 94.05% identity with the reference sequences. Among them, the 5' and 3' ends showed high identity, however, significant differences were observed in the middle sequences, including long-fragment insertions in some genes, likely due to varietal differences between the source of the reference genome and the cloned material.

3.2. Protein Physicochemical Properties and Structural Analysis of the LjDFR Gene Family

Analysis of the physicochemical properties of the cloned LjDFR proteins revealed variations in length, ranging from 328 amino acids (LjDFR3, LjDFR4) to 391 amino acids (LjDFR2), with an average length of 350.5 amino acids (Table S2). Molecular weights ranged from 36.693 kDa (LjDFR4) to 43.686

 doi:10.20944/preprints202511.1484.v1

kDa (LjDFR2), and the theoretical isoelectric point (pI) ranged from 5.82 (LjDFR2) to 8.28 (LjDFR5). The grand average of hydropathicity (GRAVY) values were all negative, indicating that all LjDFR proteins are hydrophilic. Subcellular localization prediction suggested that LjDFR1-LjDFR5 are localized in the cytoplasm, while LjDFR6 is nuclear (Table S2).

Secondary structure prediction indicated that all family members contain α-helix, β-turn, random coil, and extended strand (Figure 2A). Except for LjDFR2 (random coil > α-helix > extended strand > β-turn), the order of prevalence was α-helix > random coil > extended strand > β-turn. Notably, LjDFR4 has the highest α-helix content at 42.07%, and LjDFR5 has the lowest at 39.35%; LjDFR2 has the highest random coil content at 40.15%, and LjDFR4 has the lowest at 34.76%; LjDFR3 and LjDFR4 have the highest extended strand content at 15.55%, and LjDFR6 has the lowest at 13.05%; LjDFR4 has the highest β-turn content at 7.62%, and LjDFR6 has the lowest at 6.79% (Figure 2A). The tertiary structure is shown in Figure 2B, the proportions of α-helix and random coil in LjDFR family members are large, consistent with the secondary structure prediction results. The space enclosed by inversely parallel β-sheets of varying sizes in the middle can bind to specific DNA sequences (Figure 2B). Transmembrane structure prediction results showed that only LjDFR2 among the LjDFR family members contains 1 transmembrane domain (1-6 aa), with the N-terminus located intracellularly (7-24 aa) and the C-terminus located extracellularly, making it a transmembrane protein. Other LjDFR members do not contain transmembrane domains (Figure 2C).

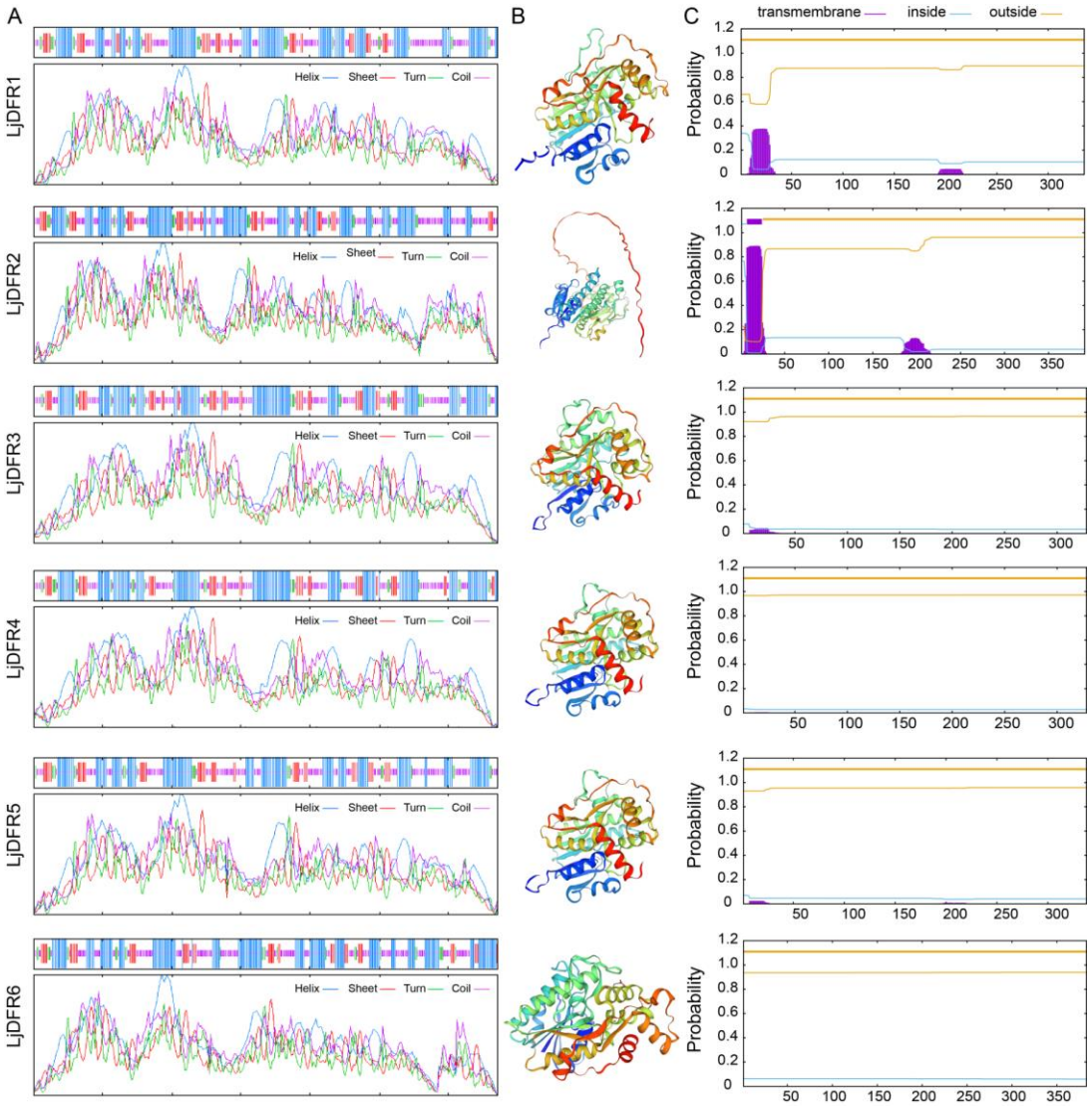

Figure 2. Prediction of secondary structure (**A**), tertiary structure (**B**) and transmembrane structure (**C**) of LjDFR proteins.

 doi:10.20944/preprints202511.1484.v1

3.3. Subcellular Localization Analysis of LjDFR Proteins

To experimentally verify subcellular localization, recombinant 35S::LjDFR3-GFP and 35S::LjDFR6-GFP plasmids were constructed and transiently expressed in tobacco epidermal cells. The control (35S::GFP) showed diffuse fluorescence throughout the nucleus, cell membrane, and cytoplasm (Figure 3). In contrast, the fluorescence signals of 35S::LjDFR3-GFP and 35S::LjDFR6-GFP were mainly distributed in the cell membrane and nucleus, overlapping with the respective markers, resulting in color changes (Figure 3). This confirms that both LjDFR3 and LjDFR6 proteins are localized to the cell membrane and nucleus.

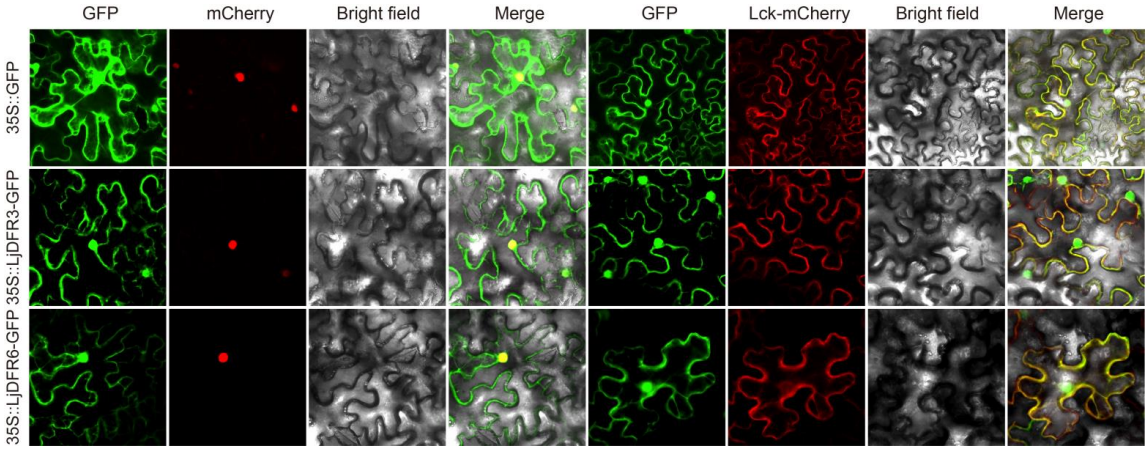

Figure 3. Subcellular localization of LjDFR proteins. GFP indicates the green fluorescence field, mCherry stands for the nuclear marker, Luc-mCherry stands for the membrane marker, Bright field indicates the bright field images, and Merge stands for the superimposed field. Scale bar =20 μm.

3.4. Phylogenetic Analysis of the LjDFR Family

To investigate the evolutionary conservation of *LjDFR* genes, we performed multiple sequence alignment. The N-terminal region of LjDFR proteins contains a highly conserved putative NADPH-binding motif, while the C-terminal regions are more variable (Figure S1). Based on the residue at position 134, LjDFR2 belongs to the Asn-type, whereas the other five LjDFR proteins belong to the non-Asn/non-Asp type (Figure S1).

Phylogenetic analysis with DFR proteins from four other species classified the LjDFR proteins into four subfamilies (Groups I-IV), all clustering with DFRs from other species, indicating that LjDFR proteins are highly conserved in higher plant evolution. Among them, no LjDFR proteins belonged to Group Ⅰ; two belonged to Group Ⅱ, which has the fewest members; one to Group Ⅲ, and three to Group IV (Figure 4).

 doi:10.20944/preprints202511.1484.v1

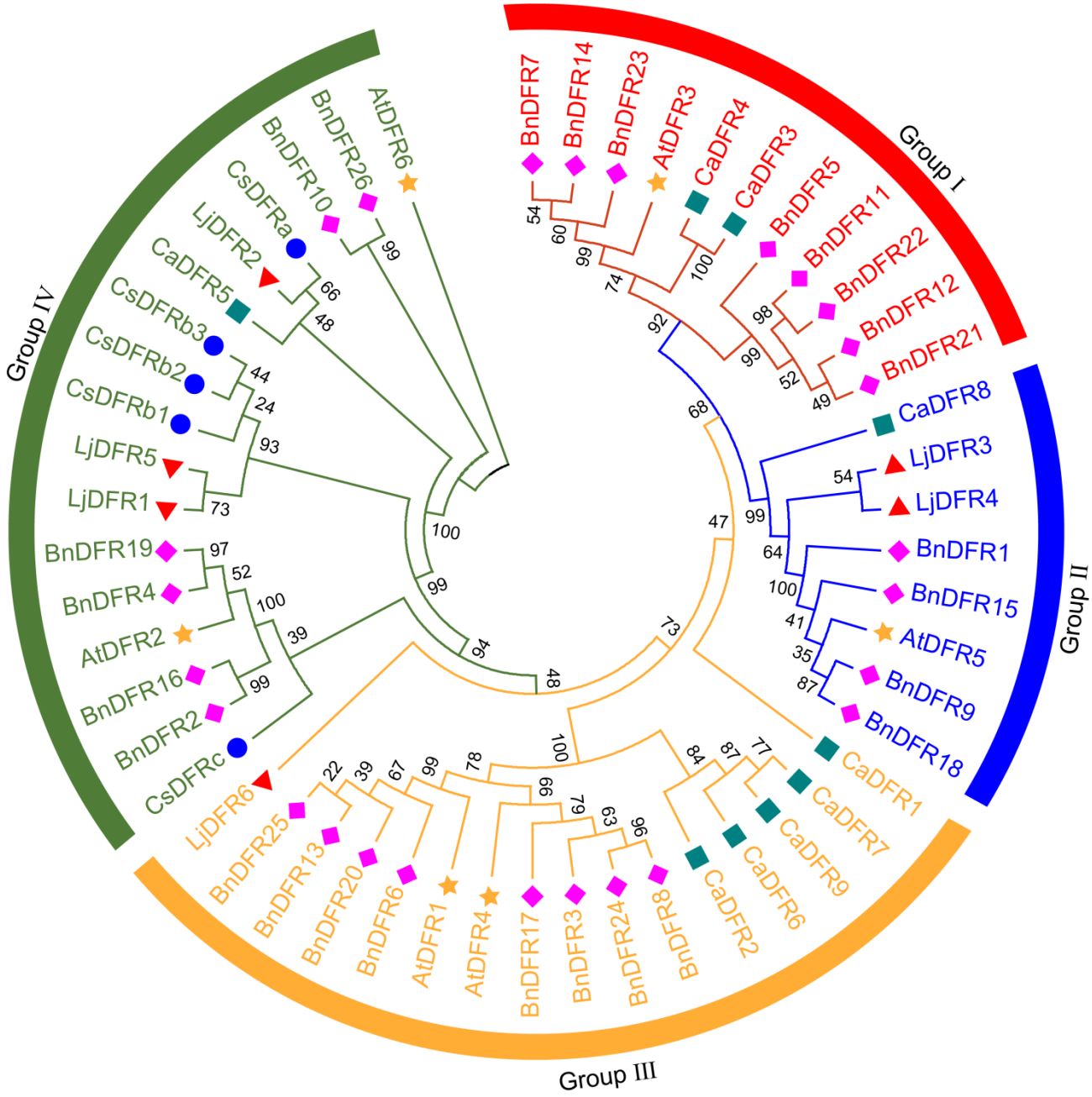

Figure 4. Phylogenetic tree of DFRs in *Lonicera japonica* (Lj, ▲), *Camellia sinensis* (Cs, ●), *Capsicum annuum* (Ca, ■), *Brassica napus* (Bn, ♦) and *Arabidopsis thaliana* (At, ★).

3.5. Gene Structure, Conserved Motifs, and Synteny Analysis of the LjDFR Gene Family

To gain deeper insight into the evolutionary relationships and structural characteristics of LjDFR proteins, analysis of conserved motifs and gene structures was performed in conjunction with the phylogenetic tree (Figure 5A). The types and numbers of motifs were highly similar within the same subgroup but varied between different subgroups. LjDFR1 and LjDFR5 contained motifs 1–9, only missing motif10; LjDFR2 contained all 10 motifs; LjDFR3 and LjDFR4 contained motifs except motif 7 and motif 9; LjDFR6 contained only motif1-6 (Figure 5B). Gene structure analysis showed that the number of exons in *LjDFR* genes ranges from 5 to 6 (Figure 5C). LjDFR5 and LjDFR6 have 5 exons, while the others have 6 exons. In summary, the similar gene structures within subgroups strongly support the reliability of the evolutionary classification.

 doi:10.20944/preprints202511.1484.v1

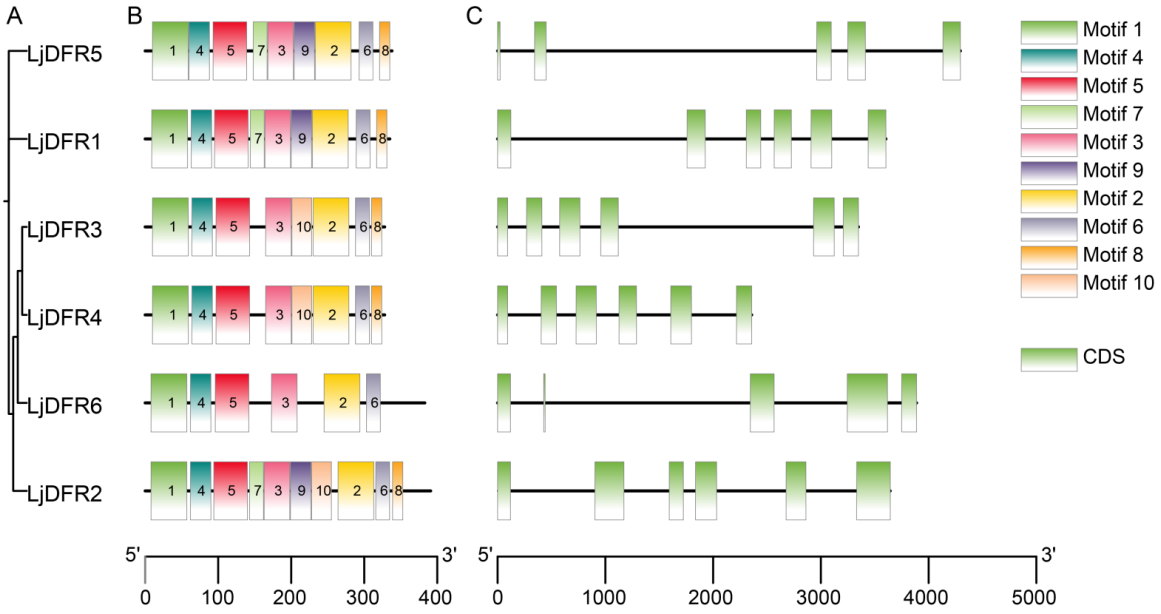

Figure 5. Phylogenetic tree (**A**), conserve motif (**B**) and gene structure (**C**) analysis of *LjDFR* gene family. (**A**) The phylogenetic tree of LjDFR proteins; (**B**) The conserved motifs of LjDFR proteins, Motif 1–10 in different colored blocks represent the motif composition; (**C**) Gene structure of *LjDFR* genes. CDS: coding sequence.

Gene duplication events play a crucial role in biological evolution. New genes produced by gene duplication may confer new functions or traits to organisms, thereby promoting species evolution and development. Collinearity analysis of gene families can help us understand the evolutionary relationships and correlations between genes in genomes or chromosomes, and reveal gene duplication events. In this study, collinearity analysis revealed no collinear relationships among the *LjDFR* genes (Figure S2). This indicates that the absence of recent gene duplication events within this family in L. japonica, the family may adopt a more flexible and rapid evolutionary strategy to help organisms adapt to the environment, and the evolutionary history of this family is full of duplications, losses, and rearrangements.

3.6. Analysis of Cis-Acting Elements in the Promoters of LjDFR Genes

Analysis of the 2,000 bp promoter regions upstream of the *LjDFR* genes identified a total of 148 *cis*-acting elements belonging to 31 types, which were categorized into four major groups (Figure 6). Light-responsive elements, including 14 types, Box4 was the most abundant (12.16% of total elements). Stress-responsive elements, including 6 types, the antioxidant response element ARE was the most numerous (6.76%). Hormone-responsive elements, including 7 types, the abscisic acid-responsive element ABRE was the most abundant (8.11%). Elements related to plant growth and development, including 4 types, O2-site was the most numerous (2.70%). Notably, *LjDFR1* lacked hormone-responsive elements, while all other *LjDFR* promoters contained all 4 types. In addition, The specific composition of major elements varied among genes (e.g., *LjDFR1* rich in TCT-motif; *LjDFR2*, *LjDFR4*, *LjDFR6* rich in Box 4; *LjDFR3* rich in G-Box, GATA-motif, ABRE, ARE, MBS; *LjDFR5* rich in TC-rich repeats) (Figure 6). These results suggest that *LjDFR* genes may be involved in processes such as photosynthesis, growth, development and responses to various hormones and abiotic stresses.

 doi:10.20944/preprints202511.1484.v1

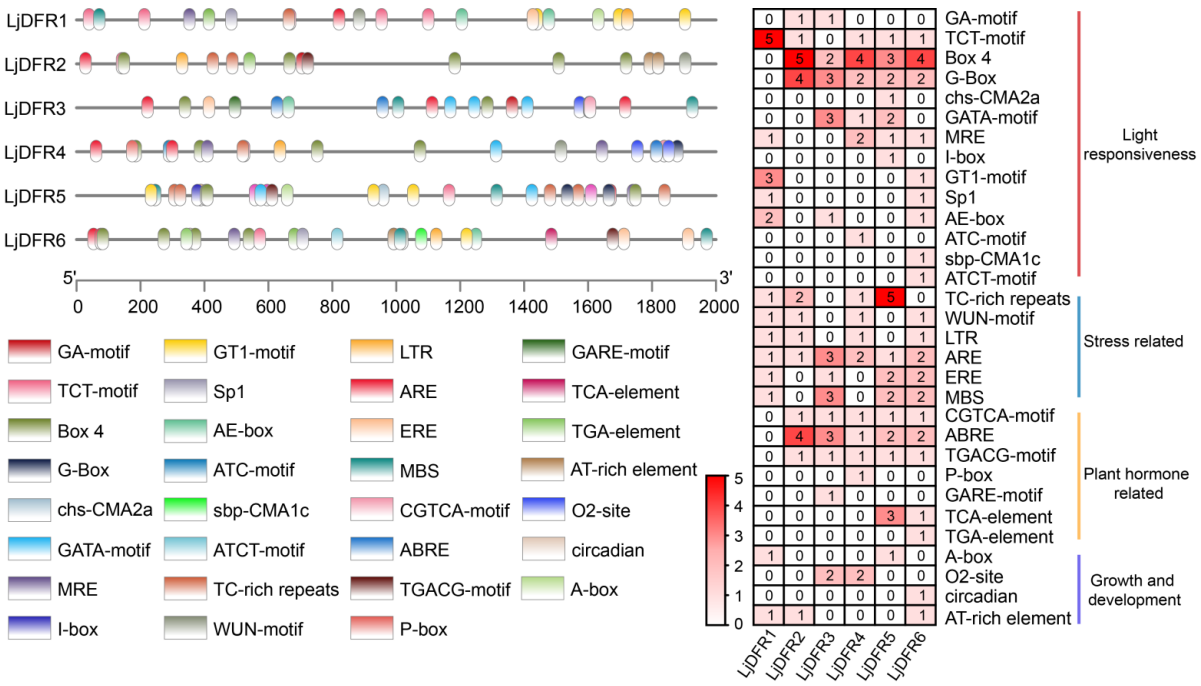

Figure 6. *Cis*-elements in the *LjDFR* gene promoters. (**A**) The location of the promoter *cis*-acting elements. (**B**) Statistical analysis of number of *cis*-acting elements in promoter region of *LjDFR* gene family.

3.7. Tissue Expression Patterns of the LjDFR Gene Family

The qRT-PCR analysis showed that the expression of *LjDFR* genes exhibited obvious tissue specificity and was expressed in all tissues of both GFLJ and RFLJ (Figure 7). Specifically, *LjDFR1* showed the highest expression level in the flowers of GFLJ and the leaves of RFLJ; *LjDFR6* exhibited the highest expression level in the leaves of both GFLJ and RFLJ; *LjDFR2*, *LjDFR3*, and *LjDFR4* had the highest expression in the flowers of both GFLJ and RFLJ; *LjDFR5* had the highest expression in the stems of GFLJ and the roots of RFLJ (Figure 7).

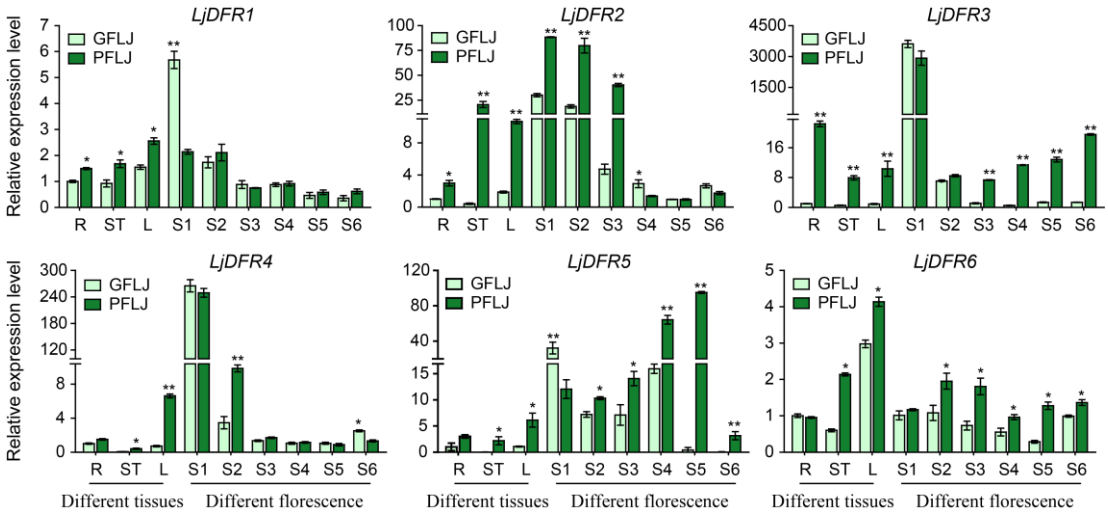

Figure 7. Differential expression patterns of *LjDFR* genes in different tissues and different florescence petals in GFLJ and RFLJ. All the data indicate means ±SD of three replicates. *indicates $P < 0.05$, **indicates $P < 0.01$.

To investigate the potential role of *LjDFR* genes in the formation of L. japonica flower color, the expression patterns of *LjDFR* genes at different flower developmental stages (S1-S6) of GFLJ and RFLJ were analyzed. The results showed that the expression patterns of *LjDFR* genes varied during flower development (S1-S6). For instance, *LjDFR1* expression gradually decreased from S1; *LjDFR2*, *LjDFR3*,

 doi:10.20944/preprints202511.1484.v1

and *LjDFR4* expression generally decreased initially and then increased, with lowest levels at S5, S4/S3, and S5, respectively; *LjDFR5* expression showed a decrease-increase-decrease trend, lowest at S6; *LjDFR6* expression exhibited an increase-decrease-increase pattern, with lowest levels at S5/S4 (Figure 7).

Comparing expression between GFLJ and RFLJ, the expression levels of all *LjDFR* genes in the stems and leaves of RFLJ were significantly higher than in GFLJ. In addition, *LjDFR2* expression in RFLJ was extremely significantly higher at S1-S3 than in GFLJ; *LjDFR3* in RFLJ was higher at S3-S6; *LjDFR4* was higher at S2; and *LjDFR5* and *LjDFR6* were significantly higher at S2-S6 (Figure 7).

3.8. Expression Patterns of the LjDFR Gene Family under Drought and Salt Stress

To investigate the response of *LjDFR* genes to drought and salt stress, the expression patterns of *LjDFR* genes under drought stress (25% PEG 6000) and salt stress (300 mmol·L^{-1} NaCl) were analyzed. The results showed that there were differences in the expression of these family members after stress exposure. Under drought stress, *LjDFR2*, *LjDFR4*, and *LjDFR5* were upregulated to varying degrees during the treatment (Figure 8). The expression level of *LjDFR2* showed a increase-decrease-increase trend. After 3 hours of stress, *LjDFR2* expression increased sharply, reaching 1.2 fold of the control, decreased thereafter, tnen was significantly lower at 48 h, and showed slight upregulation at 72 h. *LjDFR4* expression decreased initially, peaked at 48 h (2.4-fold), and then decreased. *LjDFR5* expression increased and peaked at 12 h (2.3-fold) before declining. In contrast, *LjDFR1*, *LjDFR3*, and *LjDFR6* were downregulated throughout the treatment period, and the change trends of their relative expression levels were basically consistent.

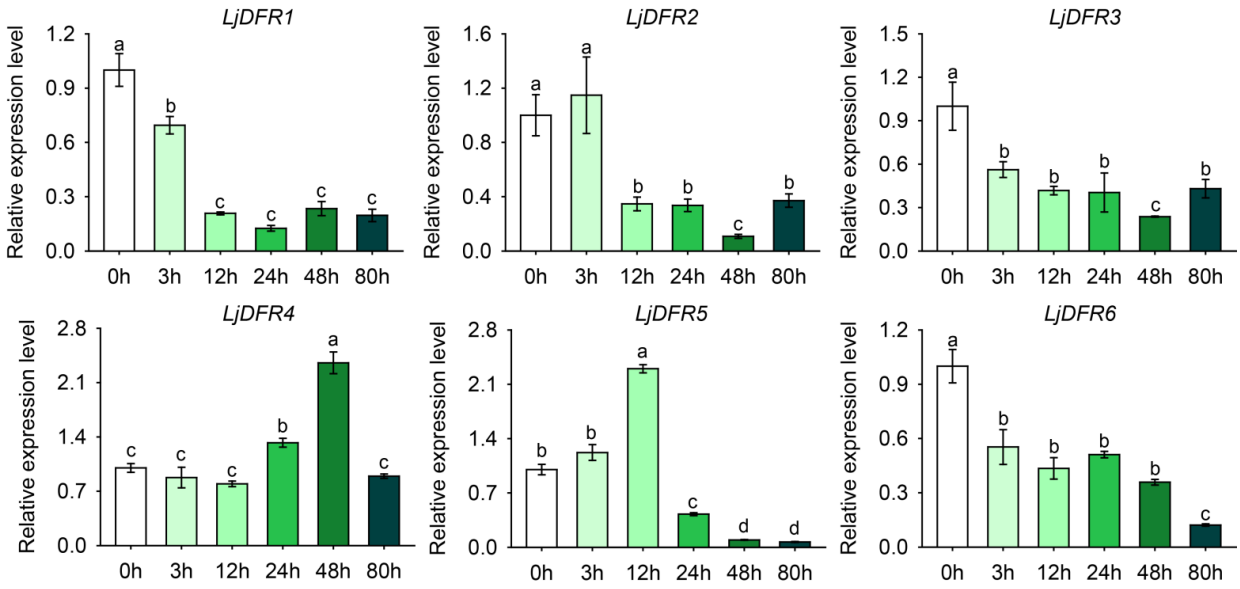

Figure 8. Expression patterns of *LjDFR* genes in L. japonica under drought treatment. All the data indicate means ±SD of three replicates. Different letters represented significant difference in purity (P<0.05).

Under salt stress, *LjDFR2*, *LjDFR4*, and *LjDFR6* were upregulated (Figure 9). The expression level of *LjDFR2* decreased initially and then increased, peaking at 72 h, which was 2.5 fold of the control. *LjDFR4* expression increased sharply at 3 h, then decreased, and reached its maximum at 24 h (3.6 fold). *LjDFR6* expression rose sharply at 3 h (2.1 fold), followed by a gradual decrease. *LjDFR1*, *LjDFR3*, and *LjDFR5* all exhibited downregulated expression to varying degrees during the treatment period (Figure 9).

 doi:10.20944/preprints202511.1484.v1

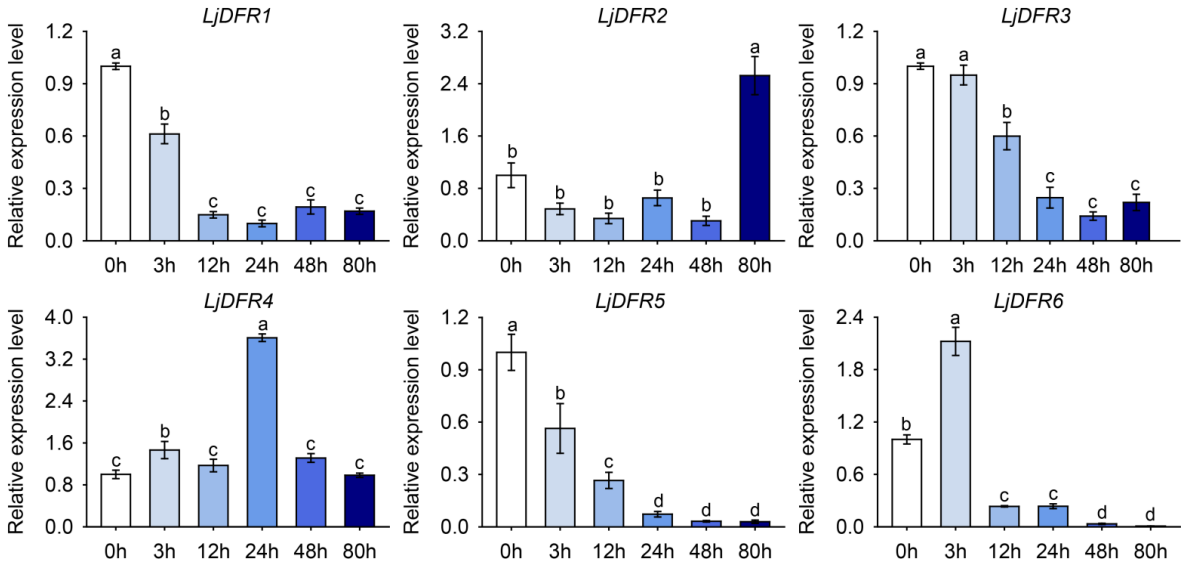

Figure 9. Expression patterns of *LjDFR* genes in L. japonica under NaCl treatment. All the data indicate means ±SD of three replicates. Different letters represented significant difference in purity (P<0.05).

4. Discussion

Flower color is a key ornamental trait and a primary target for breeding. It is mainly determined by the accumulation and combination of pigments such as chlorophyll, carotenoids, and anthocyanins [2]. DFR as the first key enzyme committed to anthocyanin biosynthesis, plays a pivotal role. Its functional loss prevents anthocyanin production, directly affecting color. The first *DFR* gene was identified in maize research and has been successfully applied in genetic engineering studies to alter the flower color of petunias [23]. In addition, overexpression of *HvDFR* in tobacco deepened the flower color of tobacco [24], overexpressing *OjDFR1* in *AtDFR* mutant tt3-1 successfully restored anthocyanin content and heterologous expression of *OjDFR1* in transgenic tobacco led to darker flower color by upregulating the expression of endogenous *NtANS* and *NtUFGT* [25], transgenic expression of *RdDFR1* restored the anthocyanin biosynthesis defects in the seed coat, hypocotyls, and cotyledons of tt3-1 and changed the flower color of tobacco from pale pink to deep pink [26]. This study identified six *DFR* genes in L. japonica, a number comparable to families in *Camellia sinensis* (5 members) [17] but smaller than in *Capsicum annuum* (9 members) [16].

The structure of *DFR* genes is associated with their functions. The length of the amino acid sequences of DFR proteins in L. japonica ranges from 328 to 391 amino acids, with an average molecular weight of 39.241 kDa, which is comparable to the length of DFR amino acid sequences reported in most other plant species [27]. The number of neutral amino acids is much larger than the number of acidic and basic amino acids, which may be more conducive to the formation of α-helix secondary structures. The α-helix content of all 6 LjDFR proteins is over 39%, and except for LjDFR2, the α-helix is the most abundant secondary structure among the other 5 LjDFR proteins. The folding pattern of a protein determines its function by influencing its shape, surface characteristics, and spatial structure. All members of the *LjDFR* gene family are hydrophilic and unstable proteins, which may be related to their relatively high proportions of α-helix and random coil structures [28]. Similar DFR structures have also been found in *Brassica oleracea*, *Glycine max*, *Meconopsis* [29–31].

In addition, the function of DFR is also related to its site of action. Subcellular localization experiments showed that LjDFR3 and LjDFR6 are localized to the cell membrane and nucleus, similar to DFRs in *Hosta ventricosa* [24] and *Brassica oleracea* [32], but differing from the cytoplasmic localization in *Loropetalum chinense* [33,34], indicating diverse subcellular localization patterns for DFRs across species. Studies have shown that anthocyanins are mainly synthesized in the cytoplasm and then transported to vacuoles for storage via transport proteins. This suggests that *DFR* genes may play roles in multiple organelles.

 doi:10.20944/preprints202511.1484.v1

Phylogenetic analysis grouped LjDFRs into four subfamilies, showing high conservation and clustering with DFRs from other species, similar to the pattern in *Capsicum annuum* [16], indicating that there are no members with species-specific evolution in L. japonica. Eukaryotic organisms undergo frequent gene duplication events during evolution. These events generate new genes for organisms, thereby helping plants adapt to environmental conditions and providing a rich genetic basis [35]. Further collinearity analysis showed that there is no collinearity among *LjDFR* genes, suggesting that there are almost no gene duplication events among members of the LjDFR family during evolution. Gene structure plays a crucial role in the evolution of gene families. Studies have shown that structural differentiation contributes more to the divergence of duplicated genes and is the main reason for the rapid emergence of new functions and new genes [36]. In this study, most *LjDFR* genes possess 6 exons, while two members (*LjDFR5*, *LjDFR6*) have 5, hinting at potential functional divergence.

LjDFR genes exhibited tissue-specific and developmentally regulated expression. Most showed highest expression in flowers, followed by leaves, consistent with findings in *Hosta ventricosa* [24] and *Carthamus tinctorius* [27]. During flower development (S1–S6), most *LjDFR* genes showed gradually decreased expression from S1, lowest at S5, and a slight increase at S6, similar to the findings to *Meconopsis* [31] and *Cineraria* [37], but inconsistent with the expression pattern of *HvDFR*—which gradually increases from S1 to S3 stage of flower development and then decreases [24]. These results indicate that the expression of *DFR* genes is species- and stage-specific regulation.

Crucially, the expression levels of *LjDFR* genes were generally higher in the red-flowered variety (RFLJ) than in the green-flowered (GFLJ), particularly in pigmented tissues and specific developmental stages, such as stems, leaves and some flowering periods. All *LjDFR* genes in stems and leaves of RFLJ were significantly higher than in GFLJ, the expression levels of *LjDFR2*, *LjDFR3*, *LjDFR4*, *LjDFR5* and *LjDFR6* in RFLJ were extremely significantly higher than in GFLJ at S1-S3, S3-S6, S2, S2-S6 and S2-S6 respectively. This correlation between higher *DFR* expression and darker pigmentation aligns with observations in *Rhododendron hybridum* [38] and *Chrysanthemum morifolium* [39,40]. Phylogenetically, LjDFR2 clusters closely with functionally characterized DFRs CsDFRa [17] and CaDFR5 [16]. Previous studies have confirmed that the CsDFRa protein has DFR activity and can convert dihydroflavonols into leucoanthocyanidins in vitro. Moreover, overexpression of *CsDFRa* in the *AtDFR* mutant (tt3) showed that these proteins are involved in the biosynthesis of anthocyanins and proanthocyanidins (PAs): they not only restored the purple petiole phenotype but also improved the seed coat color [17]. Additionally, the expression level of *CaDFR5* is consistent with changes in anthocyanin content [16]. This, combined with its high expression in RFLJ, strongly suggests that *LjDFR2* plays a positive role in anthocyanin accumulation and flower color formation in L. japonica.

Promoter is a DNA sequence located upstream of a gene. Gene promoters contain various *cis*-acting elements, which can function individually or collectively to enhance or inhibit transcription; they can also bind to different transcription factors to regulate the transcriptional level of genes in response to biotic or abiotic stresses. Therefore, studying gene promoters to analyze the expression characteristics and functions of plant genes is of great significance. In this study, promoter analysis revealed an abundance of stress-responsive *cis*-elements, prompting investigation under abiotic stress. Accordingly, drought and salt stress treatments were applied to L. japonica. The results showed that under drought stress, *LjDFR2*, *LjDFR4*, and *LjDFR5* all exhibited upregulated expression to varying degrees during the treatment period, reaching 1.2-fold, 2.4-fold, and 2.3-fold of the control, respectively. Under salt stress, *LjDFR2*, *LjDFR4*, and *LjDFR6* also showed upregulated expression being 2.5-fold, 3.6-fold, and 2.1-fold of the control, respectively. Among them, both *LjDFR2* and *LjDFR4* were significantly induced under drought and salt stress, indicating their potential roles in abiotic stress response, which lays a foundation for further analyzing the functions and mechanisms of *LjDFR* genes.

 doi:10.20944/preprints202511.1484.v1

5. Conclusions

In this study, six *LjDFR* genes were identified in L. japonica through genome-wide analysis. Their full-length sequences were successfully cloned and comprehensive analyses of their chromosomal location, subcellular localization, protein structure, phylogenetic relationships, promoter *cis*-elements, and expression profiles were conducted. The results demonstrate that the *LjDFR* gene family is relatively conserved and its members are involved in flower color formation and responses to drought and salt stress. Specifically, *LjDFR2* is strongly implicated in anthocyanin accumulation, while *LjDFR2* and *LjDFR4* are key responders to abiotic stress. This work provides a theoretical foundation for further functional characterization of *LjDFR* genes and offers valuable candidate genes for molecular breeding aimed at improving ornamental traits and stress resistance in L. japonica.

Supplementary Materials: The following supporting information can be downloaded at the website of this paper posted on Preprints.org. Figure S1: Multiple sequence alignment of LjDFR proteins. The NADPH-binding site is boxed in green; Figure S2: Collinearity analysis of the *LjDFR* gene family; Table S1: Primers used in this study; Table S2: Physiochemical prosperities and subcellular location analysis results of LjDFRs.

Author Contributions: Conceptualization, Zhengwei Tan, Huizhen Liang; methodology, Dandan Lu, Xiaoyu Su; software, Lei Li, Lina Wang; validation, Yiwen Cao; formal analysis, Yongliang Yu, Meiyu Qiao ; investigation, Yao Sun; resources, Mengfan Su; data curation, Yiwen Cao, Chunming Li; writing—original draft preparation, Dandan Lu; writing—review and editing, Zhengwei Tan, Xiaoyu Su; visualization, Hongqi Yang, Yiwen Cao; supervision, Huizhen Liang; project administration, Zhengwei Tan, Chunming Li ; funding acquisition, Zhengwei Tan, Huizhen Liang. All authors have read and agreed to the published version of the manuscript.

Funding: This research was funded by Key Research and Development Program of Henan [241111310200,231111110800,251111310600, 251111111800]; Central Government-Guided Local Science and Technology Development Fund Project of Henan Province (2025ZYYD07); the China Agriculture Research System of MOF and MARA [grant number CARS-21]; Henan Agriculture Research System[HARS-22-11-G3]; Independent Innovation Projects of Henan Academy of Agricultural Sciences [2025ZC45]; Henan Academy of Agricultural Sciences Outstanding Youth Science and Technology Fund [2024YQ15,2024YQ16]; Henan Center for Overseas Scientists[GZS2024025]; the Henan Province Science and Technology Research Project [252102111079, 252102110295,252102110255].

Data Availability Statement: All data related to this study are open-access, and the databases, websites, and software information used have been detailed in the article and are available for interested researchers.

Acknowledgments: The data used to support the funding of this study are available from the corresponding author upon request.

Conflicts of Interest: The authors declare no conflict of interest.

References

1. Karanjalker, G.R.; Ravishankar, K.V.; Shivashankara, K.S.; Dinesh, M.R.; Roy, T.K.; Sudhakar Rao, D.V. A Study on the expression of genes involved in carotenoids and anthocyanins during ripening in fruit peel of green, yellow, and red colored mango cultivars. *Appl. Biochem. Biotechnol.* **2018**, 184, 140-154. https://doi:10.1007/s12010-017-2529-x
2. Shang, Y.; Venail, J.; Mackay, S.; Bailey, P.C.; Schwinn, K.E.; Jameson, P.E.; Martin, C.R.; Davies, K.M. The molecular basis for venation patterning of pigmentation and its effect on pollinator attraction in flowers of Antirrhinum. *New Phytol*. **2011**, 189, 602-615. https://doi:10.1111/j.1469-8137.2010.03498.x
3. Zhang, Y.; Butelli, E.; Martin, C. Engineering anthocyanin biosynthesis in plants. *Curr. Opin. Plant Biol.* **2014**, 19, 81-90. https://doi:10.1016/j.pbi.2014.05.011

 doi:10.20944/preprints202511.1484.v1

4. Xie, S.; Zhao, T.; Zhang, Z.W.; Meng, J.F. Reduction of dihydrokaempferol by *Vitis vinfera* dihydroflavonol 4-reductase to produce orange Pelargonidin-Type anthocyanins. *J. Agric. Food Chem.* **2018**, 66, 3524-3532. https://doi:10.1021/acs.jafc.7b05766
5. Jaakola, L. New insights into the regulation of anthocyanin biosynthesis in fruits. *Trends Plant Sci.* **2013**, 18, 477-483. https://doi:10.1016/j.tplants.2013.06.003
6. LaFountain, A.M.; Yuan, Y.W. Repressors of anthocyanin biosynthesis. *New Phytol.* 2021, 231, 933-949. https://doi:10.1111/nph.17397
7. Miyagawa, N.; Miyahara, T.; Okamoto, M.; Hirose, Y.; Sakaguchi, K.; Hatano, S.; Ozeki, Y. Dihydroflavonol 4-reductase activity is associated with the intensity of flower colors in delphinium. *Plant Biotechnol.* **2015**, 32, 249-255. https://doi:10.5511/plantbiotechnology.15.0702b
8. Ni, J.; Ruan, R.J.; Wang, L.J.; Jiang, Z.F.; Gu, X.J.; Chen, L.S.; Xu, M.J. Functional and correlation analyses of dihydroflavonol-4-reductase genes indicate their roles in regulating anthocyanin changes in *Ginkgo biloba*. *Ind. Crops Prod.* **2020**, 152, 112546. https://doi:10.1016/j.indcrop.2020.112546
9. Johnson, E.T.; Ryu, S.; Yi, H.; Shin, B.; Cheong, H.; Choi, G. Alteration of a single amino acid changes the substrate specificity of dihydroflavonol 4-reductase. *Plant J.* **2001**, 25, 325-333. https://doi:10.1046/j.1365-313x.2001.00962.x
10. Liu, H.L.; Lou, Q.; Ma, J.R.; Su,B.B.; Gao, Z.Z.; Liu, Y.L. Cloning and functional characterization of dihydroflavonol 4-reductase gene involved in anthocyanidin biosynthesis of *Grape Hyacinth*. *Int. J. Mol. Sci.* **2019**, 20, 4743. https://doi:10.3390/ijms20194743
11. Vainio, J.; Mattila1, S.; Abdou, S.M.; Sipari, N.; Teeri T.H. Petunia dihydroflavonol 4-reductase is only a few amino acids away from producing orange pelargonidinbased anthocyanins. *Front. Plant Sci*. **2023**, 14, 1227219. https://doi:10.3389/fpls.2023.1227219
12. Shang, X.F.; Pan, H.; Li, M.X.; Miao, X.L.; Ding, H. *Lonicera japonica* Thunb.: ethnopharmacology, phytochemistry and pharmacology of an important traditional Chinese medicine. *J. Ethnopharmacol.* **2001**, 138, 1-21. https://doi:10.1016/j.jep.2011.08.016
13. Seo, O.N.; Kim, G.S.; Park, S.; Lee, J.H.; Kim, Y.H.; Lee, W.S.; Lee, S.J.; Kim, C.Y.; Jin, J.S.; Choi, S.K.; Shin, S.C. Determination of polyphenol components of *Lonicera japonica* Thunb. using liquid chromatography—tandem mass spectrometry: contribution to the overall antioxidant activity. *Food Chem.* **2012**, 134, 572-577. https://doi:10.1016/j.foodchem.2012.02.124
14. Yuan, Y.; Yang, J.; Yu, X.D.; Huang, L.Q.; Lin, S.F. Anthocyanins from buds of *Lonicera japonica* Thunb. var. chinensis (Wats.) Bak.. *Food Res. Int.* **2014**, 62, 812-818. https://doi:10.1016/j.foodres.2014.03.026
15. Li, J.; Lian, X.; Ye, C.; Wang, L. Analysis of flower color variations at different developmental stages in two L. japonica (*Lonicera japonica* Thunb.) cultivars. *HortScience* **2019**, 54, 779-782. https://doi.org/10.21273/HORTSCI13819-18
16. An, Y.; Li, N.; Zhang, R.L.; Wang, S.; Wang, J.N. Identification and characterization of *DFR* gene family and cloning of candidate genes for anthocyanin biosynthesis in pepper (*Capsicum annuum* L.). *BMC Plant Biol.* **2025**, 25, 830. https://doi:10.1186/s12870-025-06743-z
17. Ruan, H.X.; Shi, X.X.; Gao, L.P.; Rashid, A.; Li, Y.; Lei, T.; Dai, X.L.; Xia, T.; Wang, Y.S. Functional analysis of the dihydroflavonol 4-reductase family of *Camellia sinensis*: exploiting key amino acids to reconstruct reduction activity. *Hortic. Res.* **2022**, 9, uhac098. https://doi:10.1093/hr/uhac098
18. Pu, X.D.; Li, Z.; Tian, Y.; Gao, R.R.; Hao, L.J.; Hu, Y.T.; He, C.N.; Sun, W.; Xu, M.M; Peters, R.J.; et al. The honeysuckle genome provides insight into the molecular mechanism of carotenoid metabolism underlying dynamic flower coloration. *New phytol.* **2020**, 227, 930-943. https://doi:10.1111/nph.16552
19. Lu, D.D.; Tan, Z.W.; Yu, Y.L.; Li, L.; Xu, L.J.; Yang, H.Q.; Yang, Q.; Dong, W.; An, S.F.; Liang, H.Z. Cloning, structure and expression profile analysis of *CtANR2* and *CtANR3* genes from *Carthamus tinctorius* L.. *Acta Agric. Boreali-Sin*. **2023**, 38, 84-93. https://doi:10.7668/hbnxb.20193450
20. Chen, C.J.; Chen, H.; Zhang, Y.; Thomas, H.R.; Frank, M.H.; He, Y.H.; Xia, R. TBtools: An integrative toolkit developed for interactive analyses of big biological data. *Mol Plant*. **2020**, 13, 1194-1202. https://doi:10.1016/j.molp.2020.06.009

21. Wang, Y.P.; Tang, H.B.; Debarry, J.D.; Tan, X.; Li, J.P.; Wang, X.Y.; Lee, T.H.; Jin, H.Z.; Marler, B.; Guo, H.; Kissinger, J.C.; Paterson, A.H. MCScanX: a toolkit for detection and evolutionary analysis of gene synteny and collinearity. *Nucleic Acids Res*. **2012**, 40, e49. https://doi:10.1093/nar/gkr1293
22. Liu, X.Y.; Chen, L.; Qiao, Y.G.; Rong, Y.; Wang J.S. Selection of reference genes by qRT-PCR inflower organ of *Lonicera japonica* Thunb.. *J Shanxi Agri Sci*. **2017**, 45, 514-517. https://doi:10.3969/j.issn.1002-2481.2017.04.06
23. Meyer, P.; Heidmann, I.; Forkmann, G.; Saedler, H. A new Petunia flower colour generated by transformation of a mutant with a maize gene. *Nature* **1987**, 330, 677-678. https://doi:10.1038/330677a0
24. Qin, S.; Liu, Y.T.; Cui, B.Q.; Cheng, J.L.; Liu, S.Y.; Liu, H.Z. Isolation and functional diversification of dihydroflavonol 4-Reductase gene *HvDFR* from *Hosta ventricosa* indicate its role in driving anthocyanin accumulation. *Plant signal. Behav.* **2022**, 17, e2010389. https://doi:10.1080/15592324.2021.2010389
25. Sun, W.; Zhou, N.N.; Feng, C.; Sun, S.Y.; Tang, M.; Tang, X.X.; Ju, Z.G.; Yi, Y. Functional analysis of a dihydroflavonol 4-reductase gene in *Ophiorrhiza japonica* (*OjDFR1*) reveals its role in the regulation of anthocyanin. *Peer J* **2021**, 9, e12323. https://doi:10.7717/peerj.12323
26. Sun, W.; Zhou, N.N.; Wang, Y.H.; Sun, S.Y.; Zhang, Y.; Zhigang Ju, Z.G.; Yi, Y. Characterization and functional analysis of *RdDFR1* regulation on flower color formation in *Rhododendron delavayi*. *Plant Physiol. Biochem.* **2021**, 169: 203-210. https://doi:10.1016/j.plaphy.2021.11.016
27. Tan, Z.W.; Lu, D.D.; Li, L.; Yu, Y.L.; Xu, L.J.; Dong, W.; Yang, H.Q.; Yang, Q.; Li, C.M.; Liang, H.Z. Cloning and expression analysis of dihydroflavonol 4-reductase gene from Safflower (*Carthamus tinctorius* L.). *Mol Plant Breeding*. **2022**, 20, 5309-5318. https://doi:10.13271/j.mpb.020.005309
28. Yang, C.L.; Li, Y.Z.; He, L.L.; Song, Y.H.; Zhang, P.; Liu, Z.X.; Li, P.H.; Liu, S.J. Genome-wide identification and analysis of *TPS* gene family and functional verification of *VvTPS4* in the formation of monoterpenes in Grape. *Sci Agric Sin*. **2025**, 58, 1397-1417. https://doi:10.3864/j.issn.0578-1752.2025.07.012
29. Feng, X.; Zhang, Y.T.; Wang, H.; Tian, Z.D.; Siyao Xin, S.Y.; Zhu, P.F. The dihydrofavonol 4-reductase *BoDFR1* drives anthocyanin accumulation in pink-leaved ornamental kale. *Theor. Appl. Genet.* **2021**, 134, 159-169. https://doi.org/10.1007/s00122-020-03688-9
30. Shi, Z.; Li, H.; Gao, M.; Guo, C.H.; Guo, D.L.; Bi, Y.D. Cloning of *GmDFR* gene from Soybean (*Glycine max*) and identification of its function on resistance to iron deficiency. *J. Agric. Biotechnol.* **2023**, 31, 259-272. https://doi:10.3969/j.issn.1674-7968.2023.02.005
31. Wang, H.J.; Chen, X.J.; Li, T.J.; Luo, J.; Qu, Y. Cloning and expression analysis of *DFR* gene from *Meconopsis* with different colors. *Acta Agric Boreali Sin*. **2024**, 39, 88-95. https://doi:10.7668/hbnxb.20194661
32. Zheng, H.; Zhang, F.; Jian, Y.; Huang, W.L.; Liang, S.; Jiang, M.; Yuan, Q.; Wang, Q.M.; Sun, B. Cloning and function identification of Dihydroflavonol 4-Reductase gene *BoaDFR* in *Chinese Kale*. *Acta Hortic. Sin.* **2021**, 48, 73-82. https://doi:10.16420/j.issn.0513-353x.2020-0378
33. Zhang, B.Y.; Li, C.H.; Liu, X.; Liao, X.S.; Rong, D.Y. Cloning and subcellular localization analysis of *LcDRF1* and *LcDRF2* in *Loropetalum chinense* var. rubrum. *J. South. Agric.* **2020**, 51, 2865-2874. https://doi:10.3969/j.issn.2095-1191.2020.12.001
34. Zhu, Y.; Peng, Q.Z.; Li, K.G.; Xie, D.Y. Molecular cloning and functional characterization of a dihydroflavonol 4-reductase from *Vitis bellula*. *Molecules* **2018**, 23, 861. https://doi:10.3390/molecules23040861
35. Zhou, X.Z.; Yao, S.H.; Li, J.W.; Chen, K.Y.; Yu, D. Analyses of gene duplication and synteny in *Melampsora larici-populina* (Pucciniales, Basidiomycota). *Mycosystema* **2021**, 40, 580-591. https://doi:10.13346/j.mycosystema.200345
36. Xu, G.X.; Guo, C.C.; Shan, H.Y.; Kong, H.Z. Divergence of duplicate genes in exon-intron structure. *Proc. Natl. Acad. Sci. U.S.A.* **2012**, 109, 1187-1192. https://doi:10.1073/pnas.1109047109
37. Hu, K.; Meng, L.; Han, K.T.; Sun, Y.; Dai, S.L. Isolation and expression analysis of key genes involved in anthocyanin biosynthesis of *Cineraria*. *Acta Hortic. Sin*. **2009**, 36, 1013-1022. https://doi:10.16420/j.issn.0513-353x.2009.07.008
38. Jiang, B.X.; Wang, Q.H.; Yang, G.X.; Jia, Y.H.; Xie, X.H.; Wu, Y.Y. Cloning and analysis of *RhDFR* gene in *Rhododendron hybridum* Hort.. *Acta Bot. Boreat. Occident. Sin.* **2023**, 43, 10-20. https://doi:10.7606/j.issn.1000-4025.2023.01.0010

 doi:10.20944/preprints202511.1484.v1

39. Yu, X; Li, Y.H.; Zhang, L.Y.; Liu H.; Luo C.; Cheng X.; Gao K.; Huang C.L.; Chen D.L. Cloning and expression analysis of *CmDFRa* gene in *Chrysanthemum* × *morifolium*. *Mol Plant Breeding*. **2024**, 4, 1-13. https://link.cnki.net/urlid/46.1068.S.20240424.0948.005
40. Lim, S.H.; Park, B.; Kim, D.H.; Park, S.; Yang, J.H.; Jung J.A.; Lee J.M.; Lee J.Y. Cloning and functional characterization of dihydroflavonol 4-reductase gene involved in anthocyanin biosynthesis of *Chrysanthemum*. *Int. J. Mol. Sci*. **2020**, 21, 7960. https://doi:10.3390/ijms21217960